Nucleic Acids Research, 2013, **1–14**
doi:10.1093/nar/gkt060

The RNA exosome complex central channel controls both exonuclease and endonuclease Dis3 activities *in vivo* and *in vitro*

Karolina Drążkowska[1,2], Rafał Tomecki[1,2], Krystian Stoduś[1,2], Katarzyna Kowalska[1,2], Mariusz Czarnocki-Cieciura[1,2] and Andrzej Dziembowski[1,2,*]

[1]Department of Biophysics, Institute of Biochemistry and Biophysics, Polish Academy of Sciences, Pawińskiego 5a, 02-106 Warsaw, Poland and [2]Faculty of Biology, Institute of Genetics and Biotechnology, University of Warsaw, Pawińskiego 5a, 02-106 Warsaw, Poland

Received September 25, 2012; Revised December 21, 2012; Accepted January 14, 2013

ABSTRACT

The RNA exosome is an essential ribonuclease complex involved in RNA processing and decay. It consists of a 9-subunit catalytically inert ring composed of six RNase PH-like proteins forming a central channel and three cap subunits with KH/S1 domains located at the top. The yeast exosome catalytic activity is supplied by the Dis3 (also known as Rrp44) protein, which has both endo- and exoribonucleolytic activities and the nucleus-specific exonuclease Rrp6. *In vitro* studies suggest that substrates reach the Dis3 exonucleolytic active site following passage through the ring channel, but *in vivo* support is lacking. Here, we constructed an Rrp41 ring subunit mutant with a partially blocked channel that led to thermosensitivity and synthetic lethality with Rrp6 deletion. Rrp41 mutation caused accumulation of nuclear and cytoplasmic exosome substrates including the non-stop decay reporter, for which degradation is dependent on either endonucleolytic or exonucleolytic Dis3 activities. This suggests that the central channel also controls endonucleolytic activity. *In vitro* experiments performed using *Chaetomium thermophilum* exosomes reconstituted from recombinant subunits confirmed this notion. Finally, we analysed the impact of a lethal mutation of conserved basic residues in Rrp4 cap subunit and found that it inhibits digestion of single-stranded and structured RNA substrates.

INTRODUCTION

The RNA exosome plays a central role in eukaryotic cell RNA metabolism by hydrolyzing RNA and is responsible for the only essential 3′ to 5′ exoribonucleolytic activity in yeast (1,2). The exosome regulates mRNA levels in the RNA turnover process and participates in different nuclear RNA processing pathways including snRNA, snoRNA, tRNA and 5.8S rRNA maturation (3) and also degrades RNA processing by-products such as 5′ External Transcribed Sequence (5′-ETS). The exosome is also involved in RNA quality control, as it degrades aberrant RNA molecules in the nucleus (rRNA, tRNA, snRNA, snoRNA) (4) and acts in cytoplasmic RNA surveillance pathways: non-stop decay (NSD), degrading mRNA without a termination codon; nonsense-mediated decay (NMD), degrading molecules with premature stop codons (PTC) and no-go decay (NGD), degrading RNA in stalled ribosomes [reviewed in (5)]. In the cytoplasm, many of these pathways are redundant with 5′ to 3′ decay mediated by decapping enzymes and Xrn1 exonuclease.

The evolutionarily conserved core of the exosome consists of a 9-subunit ring, which is catalytically inert, and the 3′–5′ RNase Dis3/Rrp44 (this assembly is referred to here as the 10-subunit exosome) (see Figure 1A) (6–8). Deletion of genes encoding any of these proteins is lethal for yeast. The ring is composed of a 6-subunit base (Rrp41, Rrp42, Rrp43, Rrp45, Rrp46 and Mtr3) and a cap formed by Rrp4, Rrp40 and Csl4 proteins (Figure 1A). The conserved central channel of the complex is composed of the base subunits. Rrp41—the most conserved of the base proteins—contains basic residues that are suspected to interact with RNA passing through the channel (9). In the nucleus, an additional RNase—Rrp6—associates with the exosome, thus forming an 11-subunit exosome complex (10). The catalytic activity of the exosome core is provided by the Dis3 protein that is both an exo- and endoribonuclease (11–13). These two nucleolytic activities are dependent on the RNase II catalytic (RNB) domain [supported by an S1 and two cold shock RNA-binding domains (CSD)] (14) and the N-terminal PilT (PIN) domain (synergistically with the CR3 motive) (15), respectively (Figure 1A).

*To whom correspondence should be addressed. Tel: +48 225922033; Fax: +48 226584176; Email: andrzejd@ibb.waw.pl

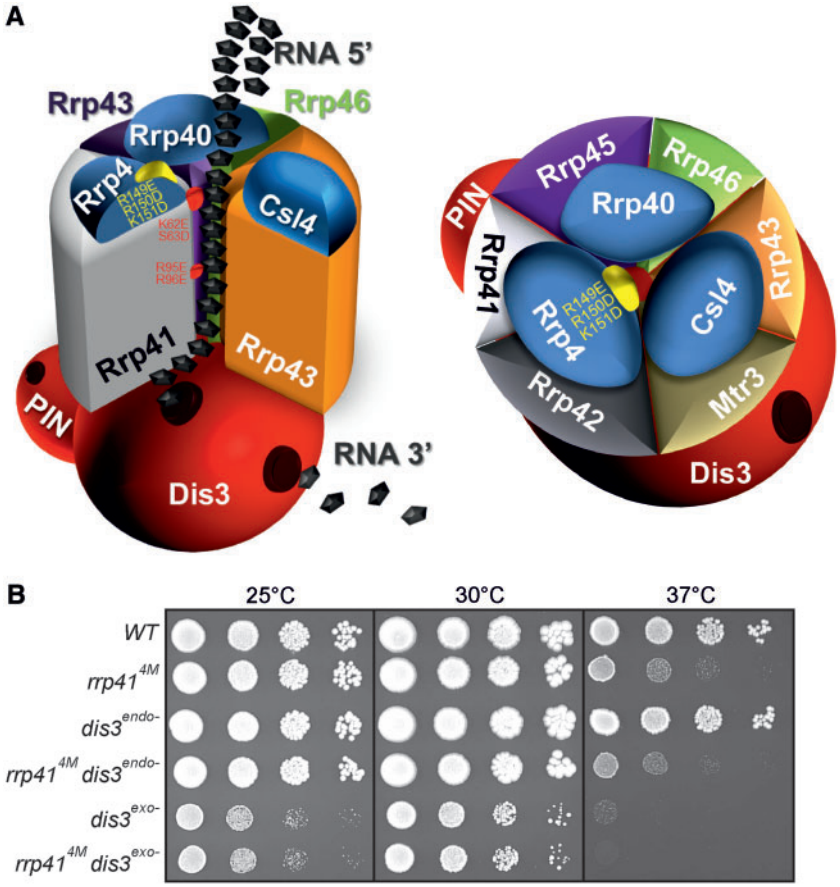

Figure 1. The *Rrp41*^{4M} mutation blocking the channel inhibits growth at elevated temperatures. (**A**) Architecture of the exosome complex. The position of mutated sites is indicated (mutated residues in Rrp41 responsible for the interaction with RNA shown in red, mutated residues in Rrp4 presumably responsible for the interaction with RNA shown in yellow). (**B**) Serial dilutions of strains: *rrp41*^{4M}, *dis3*$^{endo-}$, *rrp41*^{4M} *dis3*$^{endo-}$, *dis3*$^{exo-}$, *rrp41*^{4M} *dis3*$^{exo-}$ and an isogenic wild-type (WT) control strain were placed on YPDA plates and incubated at 25, 30 and 37°C for 3 days.

The Dis3 proteins with the same domain architecture are present in most of eukaryotes including: fungi, plants and animals. The human genome encodes two Dis3 paralogues interacting with the exosome ring: hDIS3 and hDIS3L, which display different cellular localization. The hDIS3 is present mostly in the nucleus, whereas hDIS3L is strictly cytoplasmic (16,17). Interestingly, the RNB domain of hDIS3, but not hDIS3L, is frequently mutated in multiple myeloma, suggesting that inhibition of exonucleolytic (but not endonucleolytic) activity of the nuclear exosome has some advantages for tumor growth (18).

The Dis3 protein attaches to the bottom of the exosome ring via its N-terminal PIN domain, which contacts the Rrp41 base subunit, as demonstrated by the crystal structure of the Dis3/Rrp41/Rrp45 trimer, which is supported by electron microscopy reconstructions (9,19). Recent study has shown that additional contacts between the 9-subunit ring and Dis3 are mediated by the conserved CR3 motif located upstream the PIN domain (15). Results from several *in vitro* studies suggest that RNA is threaded through the central channel to the exonucleolytic active site of Dis3: (i) the RNB domain active site was found to be positioned in close proximity to the channel exit (9,19); (ii) electron microscopy reconstruction of RNA-bound exosomes shows RNA density at the top of the channel and mutation of conserved basic residues of the Rrp4 protein near the channel entrance is lethal (19); and (iii) channel blockage resulting from substituting conserved basic residues in Rrp41 with acidic ones decreases the activity of the 10-subunit exosome, which correlates with a lack of exosome-dependent RNA protection (9). However, there are no *in vivo* data to support the role of the channel in RNA threading, and results of structural studies do not exclude the existence of alternative pathways. Furthermore, nothing is known about the possible role of the channel in controlling the PIN domain endonucleolytic activity, particularly considering that its active site is exposed to the solvent, suggesting a lack of dependence on the channel (9).

In the present study, we analysed the role of the exosome central channel in greater detail by constructing a *Saccharomyces cerevisiae* strain in which electrostatic occlusion is produced by acidic amino acid substitutions made at four conserved basic residues of Rrp41 that are exposed to the channel; a similar quadruple mutation was previously shown to inhibit 10-subunit exosome activity *in vitro* (9). We also performed *in vitro* experiments on reconstructed exosomes from the thermophilic fungus *Chaetomium thermophilum* and analysed the molecular

phenotypes and changes in exosome function caused by mutating basic residues in the Rrp4 cap subunit.

MATERIALS AND METHODS

Strain construction

The DNA fragment containing wild-type (*RRP4*^{WT}) or R149E R150D K151D (*RRP4*^{3M}) *RRP4* gene and protein A sequence was amplified by overlap polymerase chain reaction (PCR) and cloned into the pRS415 vector to generate pADZ488 and pADZ489 plasmids, respectively, which were transformed into the TH_6151 strain (20). Similarly, pADZ586 and pADZ587 were generated by introducing, respectively, the *RRP4* wild-type (*RRP4*^{WT}gfp) or R149E R150D K151D (*RRP4*^{3M}gfp) *RRP4* gene amplified in overlap PCR with an egpf (enhanced green fluorescent protein) sequence and transformed into the TH_6151 strain. Other yeast strains used in the study are listed in Supplementary Table S2. Yeast strain construction is described in Supplementary Methods.

Purification of yeast exosomes

Protein A-tagged yeast exosomes were purified by immunoglobulin G affinity purification followed by size-exclusion chromatography on a Superdex 200 Column (GE Healthcare). Exosome fractions were concentrated and stored at −20°C in 150 mM NaCl, 10 mM Tris (pH 8) and 50% (v/v) glycerol.

Confocal imaging

Cells were cultured in synthetic complete medium without leucine to an OD_{600} of 0.1–0.15 and collected by centrifuging for 2 min at 5000 rcf. Cells were resuspended in medium and mixed with 2 volumes of 1% 2-hydroxyethylagarose (Sigma). A droplet of the suspension was placed on a Superfost microscope slide (Thermo Scientific) and covered with a #1 cover glass (Marienfeld).

Imaging was performed on a FluoView FV1000 system with spectral detectors (Olympus), using a 60×/1.40 oil immersion objective lens. EGFP fluorescence was excited with the 488 nm line of an argon-ion laser and collected in the 500–600 nm range, with the confocal pinhole at 1 Airy unit. Images were processed using the Fluoview software.

Ribonuclease assays

The ss17, ss17-$(A)_2$, ss17-$(A)_3$, ss17-$(A)_4$, ss17-$(A)_{14}$, ss17-$(A)_{34}$ and compl oligoribonucleotides (sequences listed in Supplementary Table S1) were synthesized by Metabion and purified following separation in preparative 10% denaturing polyacrylamide gels as described by Lorentzen *et al.* (21). Radioactive ss17-$(A)_{14}$, ss17-$(A)_{34}$ and ds17-$(A)_{34}$ substrates, as well as ds17, ds17-$(A)_2$, ds17-$(A)_3$ and ds17-$(A)_4$ markers were prepared as discussed in Lorentzen *et al.* (21). *In vitro* enzymatic assays were essentially performed as described in (13), using reaction buffers containing 100 μM–3 mM $MgCl_2$ or $MnCl_2$. The RNA substrate concentration was 0.05–1 μM for ss17-$(A)_{34}$ in endoribonuclease and exoribonuclease assays, respectively, and 0.2 μM for ds17-$(A)_{34}$ in exoribonuclease assays. Concentration of recombinant proteins and reconstituted complexes was 0.05 μM. Reactions were carried out at 37°C and terminated at different time points by addition of loading dye containing 90% formamide and snap freezing in liquid nitrogen. Reaction products were analysed by electrophoresis in denaturing 20% polyacrylamide gels and visualized using a FUJI PhosphorImager.

Unwinding assay

The ds17-$(A)_{34}$ RNA duplex was prepared as aforementioned, except for the fact that the slight molar excess of 5′-labelled compl oligoribonucleotide was used in the annealing procedure, whereas ss17-$(A)_{34}$ sense-strand was unlabelled. Reactions were performed as for the exoribonuclease assays but were terminated by addition of one volume of the gel-loading dye [10 mM Tris–HCl (pH = 8.0), 60% glycerol, 60 mM ethylenediaminetetraacetic acid, 0.03% bromophenol blue, 0.03% xylene cyanol, 1% sodium dodecyl sulphate (SDS)]. Samples were analysed in native 15% polyacrylamide gel and visualized using a FUJI PhosphorImager.

In vivo assay for mRNA degradation

Strains transformed with *MFA2*pG and different versions of *PGK1*pG mRNA reporters under the control of a *GAL1* promoter were grown at 25°C until they reached OD_{600} 0.2–0.4 in medium with galactose and then shifted to 37°C for 1 h (to inactivate the decapping enzyme) before the addition of glucose. Aliquots were then removed at various time points. Each mRNA stability measurement was replicated three times using independent cultures. Average values of the experiments were graphed.

Analysis of non-stop *PGK*1pG reporter steady-state level

ADZY522 *rrp41*^{4M} (K62E S63D R95E R96E), ADZY531 *dis3*$^{endo-}$ (D171N), ADZY537 *rrp41*^{4M} (K62E S63D R95E R96E) *dis3*$^{endo-}$ (D171N), BSY1735 *dis3*$^{exo-}$ (D551N), ADZY724 *rrp41*^{4M} (K62E S63D R95E R96E) *dis3*$^{exo-}$ (D551N) and wild-type yeast strains were transformed with pRP1079 plasmid containing the non-stop *PGK1*pG reporter gene. Yeast was grown in medium with galactose. Samples were collected when cultures reached OD_{600} 0.2–0.4.

Northern blot analysis

RNA was fractionated by electrophoresis on a 6% polyacrylamide–urea (PAGE) or 1.2% formaldehyde–agarose gel before transfer to a Hybond N^+ membrane (GE Healthcare). Hybridizations were performed in PerfectHyb Plus hybridization buffer (Sigma). For 5′-ETS and NEL025 Cryptic Unstable Transcripts (CUT) random-primed PCR probes as described in (13) were used. For mRNA reporters containing polyG sequence, ^{32}P-labelled polyC oligonucleotide was used as a probe. For rRNA and *SCR1*, ^{32}P-labelled oligonucleotides listed in Supplementary Table S1 were used as probes.

Yeast complementation assay with Rrp41 mutant

The DNA fragment containing the *RRP41* gene was amplified by PCR and cloned into the pRS415 vector to generate the pADZ430 plasmid. K62E S63D R95E R96E *RRP41* mutations were introduced by site-directed mutagenesis generating the pADZ433 plasmid. Constructs with wild-type and mutated *RRP41* genes as well as an empty vector as a negative control were transformed into *S. cerevisiae* TH_3687 and ADZY524 strains with the *RRP41* gene under control of a tet-off promoter (20). Transformed cultures were grown in synthetic complete medium without leucine at 30°C overnight before spotting serial dilutions onto two plates in the absence or presence of doxycycline (10 μg/ml) to repress chromosomal WT *RRP41* gene expression. Cell growth was analysed after 60 h of incubation at 25, 30 and 37°C.

Exosome reconstruction

The exosome was reconstructed using a procedure similar to that described previously (22). All constructs were generated by standard procedures using a pET28 vector backbone (see Supplementary Table S3 for vector list). Dis3 and cap subunits (Rrp4, Rrp40 and Csl4) were produced as individual HIS-SUMO (6xHistidine-Small Ubiquitin-like Modifier) fusion proteins in *Escherichia coli*. Rrp41/Rrp45 and Rrp46/Rrp43 dimers were produced as dicistronic operons with a HIS-SUMO fusion attached to Rrp41 and Rrp46, respectively. The Rrp42/Mtr3 dimer was reconstructed by mixing extracts from *E. coli* expressing HIS-SUMO fusions of Rrp42 and Mtr3. All components were purified by Ni^{2+} affinity chromatography, followed by SUMO protease cleavage, desalting, a second round of Ni^{2+} affinity chromatography with collection of unbound material, and gel filtration. All steps were done automatically using an ÄKTAxpress apparatus.

RESULTS

Rrp41 mutation blocking the central exosome channel results in moderate growth phenotypes but is synthetically lethal with *RRP6* deletion

To analyse the role of the central channel in exosome function *in vivo,* we constructed a diploid yeast strain in which WT *RRP41* at the endogenous locus is replaced with its counterpart carrying the K62E, S63D, R95D, R96D quadruple mutation, herein called $Rrp41^{4M}$. A similar mutation was previously shown to disrupt RNA protection by the *in vitro* reconstituted exosome and to inhibit its exonucleolytic activity (9). Sporulation and dissection analysis revealed that this yeast strain was viable, but its growth was inhibited at elevated temperatures (Figure 1B). The $rrp41^{4M}$ strain crossed with the isogenic *rrp6Δ* strain underwent sporulation and dissection. In contrast, there were no viable spores with the double mutation, indicating that the $Rrp41^{4M}$ mutation is synthetically lethal with *RRP6* deletion. To confirm this result, we constructed *rrp6Δ* strains with endogenous *RRP41* under the control of a doxycycline-repressible promoter transformed with plasmids containing $RRP41^{WT}$ or $RRP41^{4M}$. In agreement with the previous result, and unlike $RRP41^{WT}$, $RRP41^{4M}$ does not support yeast growth in the *rrp6Δ* background once the endogenous *RRP41* copy is repressed (Supplementary Figure S1). This result suggests partial redundancy between Rrp6 activity and a functional channel that is similar to the *DIS3* D551N mutation that disrupts the exonuclease active site ($Dis3^{exo-}$) and is also synthetically lethal with *RRP6* deletion (6). However, a recent study by Wasmuth and Lima (23) demonstrated that channel blockage by enlargement of loops in Rrp41 oriented towards the channel also inhibits Rrp6 activity, what may suggest more complex relationship between the function of central channel and Rrp6.

Finally, we combined $RRP41^{4M}$ with mutations that abolish the catalytic activities of Dis3 protein D171N in the PIN domain active site ($Dis3^{endo-}$) or D551N in the RNB domain active site ($Dis3^{exo-}$). In both cases, we did not observe any synthetic interaction, which suggests that the channel and Dis3 function in the same pathway (Figure 1B).

$Rrp41^{4M}$ mutation causes accumulation of nuclear exosome substrates

To analyse the effect of $Rrp41^{4M}$ mutation on nuclear RNA metabolism, we isolated RNA from the following strains: *WT*, $rrp41^{4M}$, $dis3^{endo-}$ (Dis3 D171N mutation abolishing endonucleolytic activity), $rrp41^{4M}$ $dis3^{endo-}$, $dis3^{exo-}$ (Dis3 D551N mutation abolishing exonucleolytic activity) and $rrp41^{4M}$ $dis3^{exo-}$ and performed northern blot analysis for the 7S precursor of 5.8S rRNA and 5.8 rRNA mature form, 5′-ETS rRNA processing by-products, and cryptic unstable transcript (Figure 2). Accumulation of all tested exosome substrates occurred in $rrp41^{4M}$ strain, strongly suggesting that the central channel plays an important role in substrate recruitment. The phenotypes were not as strong as for the $Dis3^{exo-}$ mutation, suggesting that the $Rrp41^{4M}$ mutation is hypomorphic. The exception was 7S rRNA precursor, which did not accumulate in $dis3^{exo-}$ mutant. The effects of $Dis3^{exo-}$ and $Rrp41^{4M}$ mutations were not additive, which is in agreement with the growth phenotypes. Curiously, in the case of 7S RNA, $Rrp41^{4M}$ $Dis3^{exo-}$ double mutation was partially suppressing the phenotype observed for individual single mutants. $Dis3^{endo-}$ mutation did not have significant impact on analysed RNAs, but we observed a slight increase of 5′-ETS level in $rrp41^{4M}$ $dis3^{endo-}$ double mutant in comparisons with $rrp41^{4M}$ single mutant.

$Rrp41^{4M}$ mutation blocks cytoplasmic exosome-mediated RNA decay and surveillance pathways including NSD

In the cytoplasm of yeast cells, the most prominent RNA decay pathway is initiated by decapping, followed by Xrn1-mediated 5′–3′ degradation (24). Therefore, to study the effect of $Rrp41^{4M}$ mutation on cytoplasmic RNA decay and surveillance, we constructed a strain with an $Rrp41^{4M}$ mutation in the background of a Dcp^{1-2} decapping enzyme thermosensitive mutation (25). Dcp^{1-2} and dcp^{1-2} $rrp41^{4M}$ isogenic strains were

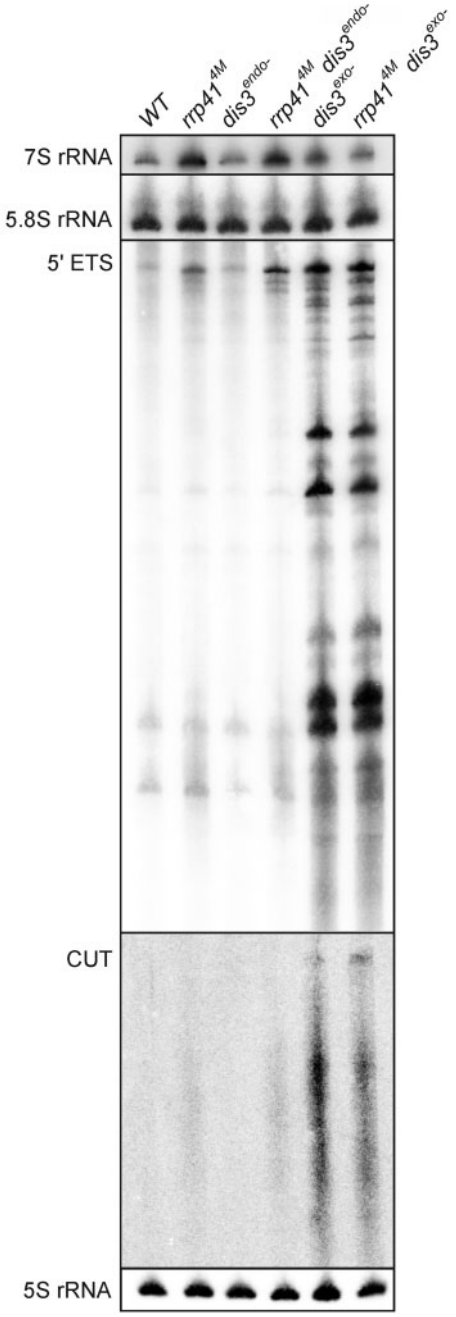

Figure 2. The *Rrp41*^{4M} mutation causes accumulation of nuclear exosome substrates. RNA from *WT*, *rrp41*^{4M}, *dis3*$^{endo-}$, *rrp41*^{4M} *dis3*$^{endo-}$, *dis3*$^{exo-}$ and *rrp41*^{4M} *dis3*$^{exo-}$ strains grown to early exponential phase was isolated and subjected to northern blot hybridizations for the following RNAs: 7S rRNA, 5.8S rRNA, 5′-ETS and CUT NEL025. The 5S rRNA was used as a loading control.

transformed with reporter constructs containing a galactose-regulated promoter and various classes of mRNAs (26): unstable *MFA2* mRNA; stable WT *PGK1* mRNA; and *PGK1* versions suspected to undergo surveillance pathways, including *PGK1* with a PTC degraded by the NMD pathway, *PGK1* with a stem-loop degraded by NGD and *PGK1* lacking the termination codon degraded by the NSD. We studied the decay of transcripts synthesized from reporters by chase experiments, where expression of the analysed gene is induced by galactose for a long time and stopped by addition of glucose to the culture media (Figure 3A–E). The *Rrp41*^{4M} mutation very strongly inhibited degradation of all analysed mRNA and resulted in much longer half lives. Surprisingly, this result was also obtained for the NSD reporter, which was previously shown to require only endo- or exonucleolytic Dis3 activity for rapid degradation (27). This finding suggests that not only the RNB exoribonuclease but also the PIN domain endoribonuclease activity of Dis3 is dependent on the central exosome channel.

NSD is mostly mediated by the exosome rather than by a 5′–3′ decay pathway (28). Therefore, to analyse the relationship between *Rrp41*^{4M} and *Dis3*$^{endo-}$ or *Dis3*$^{exo-}$ mutations, we transformed the following strains: *WT*, *rrp41*^{4M}, *dis3*$^{endo-}$, *rrp41*^{4M} *dis3*$^{endo-}$, *dis3*$^{exo-}$ and *rrp41*^{4M} *dis3*$^{exo-}$ with the NSD *PGK1* reporter plasmid and analysed the steady-state level of the reporters in yeast grown on galactose media (Figure 3F). We observed that the *Rrp41*^{4M} mutation resulted in elevated levels of the mRNA of interest, and the effect of *Dis3*$^{endo-}$ and *Dis3*$^{exo-}$ mutations was less prominent, which again supports the important role of the central exosome channel in NSD. Moreover, we noticed synergistic effect of *Rrp41*^{4M} *Dis3*$^{exo-}$ double mutation, which was not observed for nuclear exosome substrates.

Rrp41^{4M} mutation inhibits both exo- and endonucleolytic Dis3 activities *in vitro*

The results presented earlier in the text indicate that the central exosome channel controls both endo- and exoribonucleolytic Dis3 activities *in vivo*, which prompted us to perform more detailed studies *in vitro*. For this purpose, we reconstructed the 10-subunit exosome complex from *C. thermophilum* (29) (see Supplementary Table S4 for amino acid sequence alignments of *C. thermophilum* exosome subunits versus yeast and human counterparts) using recombinant subunits produced in *E. coli*. The procedure was similar to that described previously for *S. cerevisiae* (22) with minor changes (see 'Materials and Methods' section for details) and produced high yields of the *C. thermophilum* complex with high purity, which is of particular importance for the analysis of the weak PIN domain endonucleolytic activity that can be easily masked by contamination. The individual components were mixed together, purified by gel-filtration chromatography, and the successful assembly of the 10-subunit exosome was confirmed by sodium dodecyl sulphate–polyacrylamide gel electrophoresis (SDS–PAGE) (Supplementary Figure S2A). Moreover, Multi Angle Light Scattering analysis used to estimate the complex molecular weight further confirmed that the exosomes were properly assembled (Supplementary Figure S2B). We also produced exosome complexes with mutations in the Dis3 catalytic subunit at the analogous sites as those described for *S. cerevisiae* (see Supplementary Table S4), and they all assembled with comparable efficiency. In addition, we reconstructed the exosome complexes with the PIN domain alone to study the influence of the RNB domain

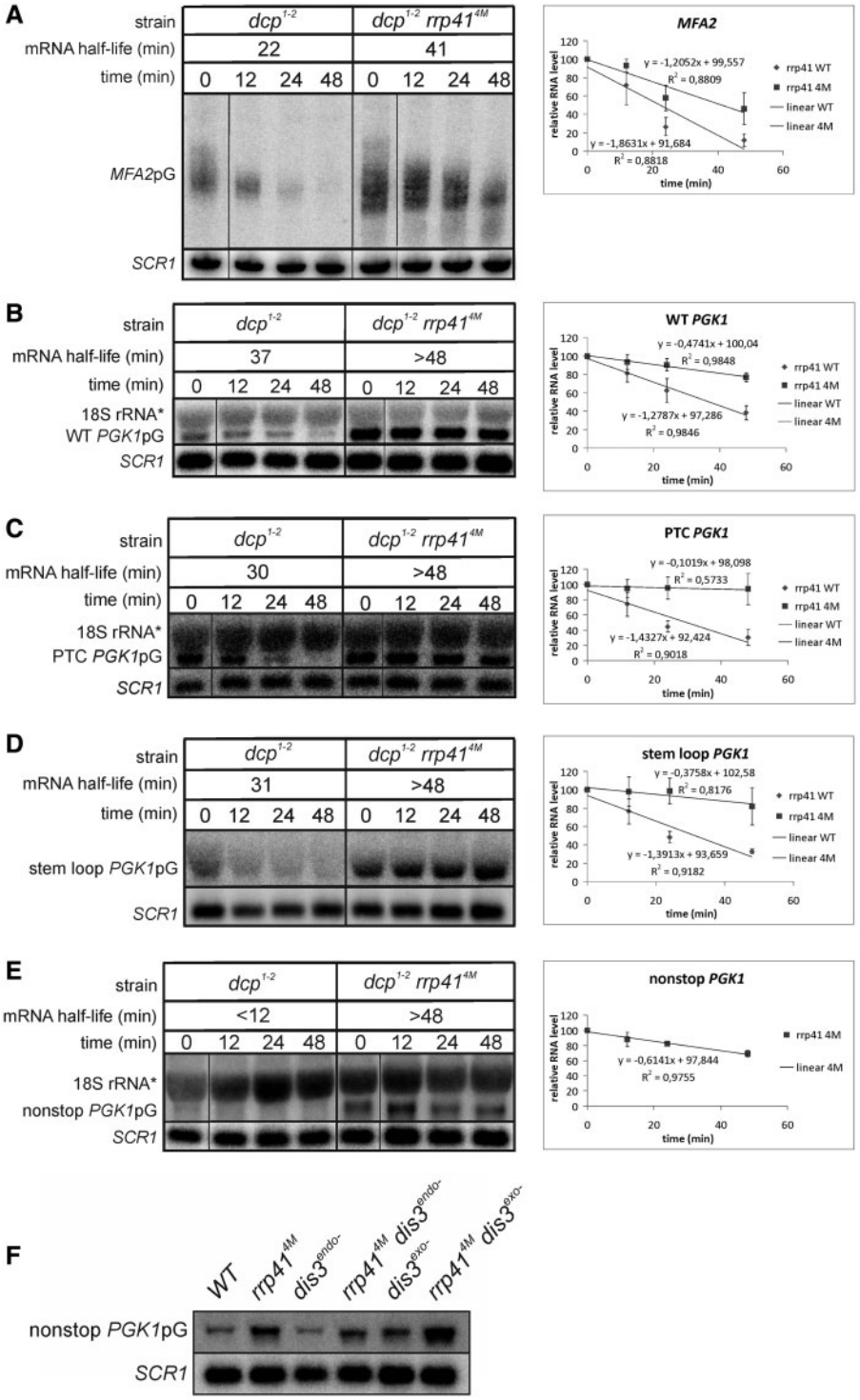

Figure 3. The *Rrp41*^{4M} mutation strongly inhibits cytoplasmic mRNA decay and surveillance. *Dcp*$^{1–2}$ and *dcp*$^{1–2}$ *rrp41*^{4M} strains were transformed with *MFA2* reporter for normal mRNA decay of short living transcript (**A**) WT *PGK1* reporter for normal mRNA decay of long living transcript (**B**) PTC reporter for analysis of NMD (**C**) *PGK1* with a stem loop structure for analysis of NGD (**D**) *PGK1* lacking a stop codon for analysis of NGD (**E**) mRNA stability in analysed strains was examined by growing cells at 25°C in galactose medium followed by a temperature shift to 37°C for 1 h and transcription termination by addition of glucose to the culture medium. RNA was isolated at the times indicated followed by northern blot analysis using a polyC probe complementary to the polyG sequence present in all reporters (upper panels). Quantifications from three independent experiments are plotted as mRNA at each time after normalization using an *SCR1* probe, and (**F**) Steady state levels of nonstop reporter in the following strains: *WT*, *rrp41*^{4M}, *dis3*$^{endo–}$, *rrp41*^{4M} *dis3*$^{endo–}$, *dis3*$^{exo–}$ and *rrp41*^{4M} *dis3*$^{exo–}$.

with S1 and CSD domains on endonucleolytic activity (Supplementary Figure S2A and C).

Purified recombinant Dis3 from *C. thermophilum* displayed similar catalytic properties as that from *S. cerevisiae*, with regard to both exoribonucleolytic (Supplementary Figure S3A and B) and endoribonucleolytic activity (Supplementary Figure S3C and D). The only difference between the two was sensitivity to magnesium ion concentration. In contrast to yeast, high [Mg^{2+}] did not significantly inhibit *C. thermophilum* exoribonucleolytic activity, whereas the endoribonucleolytic activity remained strictly dependent on a high manganese ion concentration (Supplementary Figure S4). The exoribonucleolytic activity efficiently degraded both single-stranded (Supplementary Figure S3A) and double-stranded (Supplementary Figure S3B) substrates. In the case of endoribonucleolytic activity, we observed very similar degradation patterns, irrespective of whether full-length Dis3 (Supplementary Figure S3C) or the PIN domain alone (Supplementary Figure S3D) was used in the assay. Both catalytic activities of Dis3 are strictly dependent on the aspartic acid residues present in the respective active centres of the PIN and RNB domain (Supplementary Figure S3).

Using *in vitro* reconstituted *C. thermophilum* exosomes, we first checked the effect of the channel-blocking *Rrp41*^{4M} mutation on the exonucleolytic activity by using a previously described radioactively 5′-end labelled single-stranded substrate composed of 17 generic nucleotides followed by a 34 nucleotide-long polyadenylate tail in conditions optimal for exoribonucleolytic activity (e.g. low magnesium, no manganese). The results clearly show that the blockage of the channel by the *Rrp41*^{4M} mutation strongly (~5-fold) inhibited the exoribonucleolytic activity of the exosome, which confirms the previous results (Figure 4A) (9). The effect was even more pronounced for a partially structured substrate containing a 17 nt duplex followed by a 34 nt poly(A) tail (Figure 4B). Such results corroborate well those obtained by Wasmuth and Lima (23), who also observed strong inhibition of exoribonuclease activity in the case of *in vitro* reconstituted yeast exosome on occlusion of its central channel with loops introduced into Rrp41 subunit.

Digestion of partially double-stranded substrates led to accumulation of degradation intermediate in which single-stranded extension is digested to 2–3 nucleotides, suggesting that reaction slows down when the exosome approaches closely to the secondary structure (Supplementary Figure S5). Such effect was also observed by us previously for yeast Dis3 (21) and to lower extent by others (9). We have noticed that the mutation in the endonucleolytic site seems to slightly decrease the levels of these intermediates, which we think can be explained by the slower reaction rate. However, we cannot rule out that endonucleolytic cleavages increase the level of reaction intermediate or rather by-product, which may not be further digested exonucleolytically.

We then studied Dis3 activity towards the same single-stranded substrate in conditions optimal for endoribonucleolytic activity (high manganese). We analysed the activity of reconstructed exosomes with only the Dis3 PIN domain instead of the full-length protein and noted that channel blockage significantly inhibited the endoribonucleolytic activity, similarly to the catalytic mutation in the PIN domain (Figure 5). The endonucleolytic activity was also inhibited in the context of full-length Dis3 with an exo- mutation (Figure 5). Analogous effect was observed in a recent study by Wasmuth and Lima (23). Moreover, we noticed that the endonucleolytic activity acquires some directionality in the context of the 9-subunit ring, as the very short RNA species are not visible at the beginning of the reaction as is the case of Dis3 or PIN domain alone (Figure 5 and Supplementary Figure S6). We observed that the endonucleolytic activity was highest in reconstructed exosomes with the PIN domain alone (Figure 5 and Supplementary Figure S6). To better compare the endonucleolytic activities, we performed assays for the entire exosome with wild-type PIN, exosomes with Dis3^{exo-}, PIN^{WT} alone and Dis3^{exo-} alone (Supplementary Figure S6). Again, the endonucleolytic activity of the exosome with the PIN domain alone was the highest, whereas exosomes containing full-length Dis3 with an inactive RNB domain had the lowest activity. The analysis of reconstructed exosome with the PIN domain alone instead of the full-length Dis3 was omitted in Wasmuth and Lima studies (23), what let them state that the exosome ring inhibits endonucleolytic activity. In contrast, our results suggest that the channel enhances the endonucleolytic activity, but the presence of the RNB domain in the context of the channel redirects the substrate to the RNB domain exonuclease active site, thus inhibiting the PIN domain endonucleolytic activity.

Rrp4 mutation that yields a lethal phenotype decreases degradation of both unstructured and structured substrates

In one of previous studies, we showed that triple mutation of basic residues on the surface of Rrp4, which are supposed to be involved in RNA substrate recognition by the exosome, results in a lethal phenotype (19). Here, we studied this mutation in greater detail using strains in which either a wild-type or mutant R149E, R150D and K151D version of *RRP4* (*rrp4*^{3M}) was present on centromeric plasmids, whereas the chromosomal *RRP4* copy was controlled by a doxycycline-repressible promoter, and analysed the accumulation of exosome substrates. As expected, we found that *rrp4*^{3M} behaved as a null mutant (Figure 6A). We next checked whether the *Rrp4*^{3M} mutation affects exosome activity by constructing an Rrp4 mutant strain in which the Rrp4 protein carried a TAP-tag at the C-terminus (the TAP-tag has no effect on Rrp4 function). We successfully purified the exosome complex from this strain and as with our previous studies found that the assembly of exosomes containing Rrp4^{3M} was not impaired (Figure 6B). Subsequently, we analysed digestion of a synthetic single-stranded ss17-$(A)_{14}$ RNA and partial duplex ds17-$(A)_{34}$ substrates and observed that this mutation inhibited activity by ~2–4-fold for ss17-$(A)_{14}$ (Figure 7A) and ~8-fold in the case

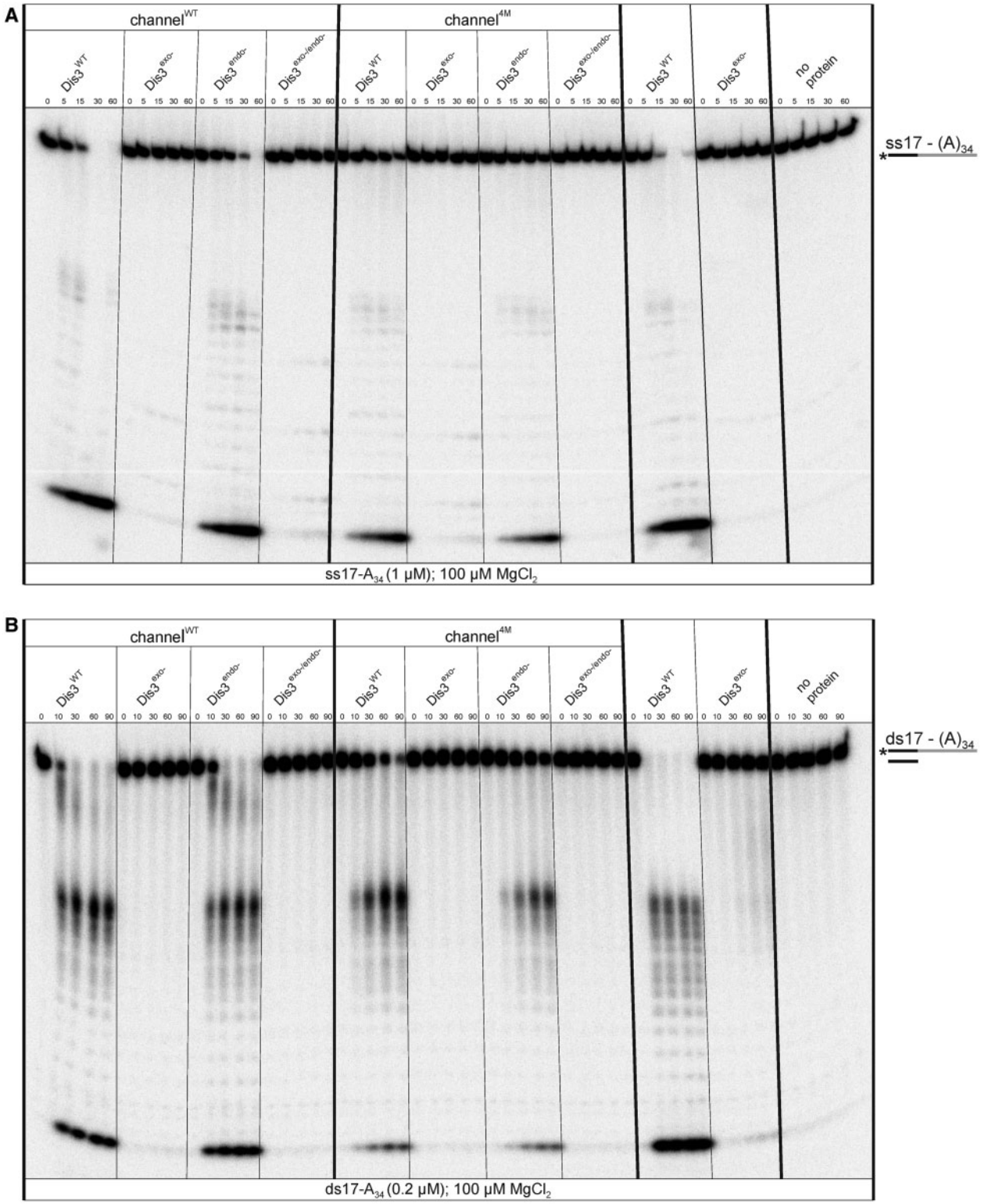

Figure 4. Exoribonucleolytic activity of Dis3 is strongly inhibited by mutations in the Rrp41 core subunit that blocks the central channel of the exosome. (**A**) 5′-labelled RNA substrates with a 17 nt generic sequence followed by a 34 adenosine tail [ss17-$(A)_{34}$] were incubated in buffer containing 100 μM magnesium with various *in vitro* reconstituted *C. thermophilum* 10-subunit exosome complexes, containing either wild-type Rrp41 or Rrp41^{4M} protein as a component of the central channel (designated channel^{WT} or channel^{4M}, respectively), in conjunction with different versions of the full-length Dis3 catalytic subunit (Dis3^{WT}, Dis3^{exo-}, Dis3^{endo-}, Dis3$^{exo-/endo-}$); parallel assays were done using individual Dis3^{WT} or Dis3^{exo-} and no added protein. Samples were collected at the indicated time points (minutes) and analysed by denaturing PAGE and phosphorimaging. Equal molar concentrations (0.05 μM) of exosome complexes or individual subunits were used for the assay. (**B**) 5′-labelled RNA substrate forming partial duplex ds17-$(A)_{34}$ (one strand consisting of 17 nucleotides generic sequence followed by a 34 adenosine-long tail and another oligo complementary to a generic sequence) was incubated in a buffer containing 100 μM magnesium with various *in vitro* reconstituted *C. thermophilum* 10-subunit exosome complexes and analysed further as in (A).

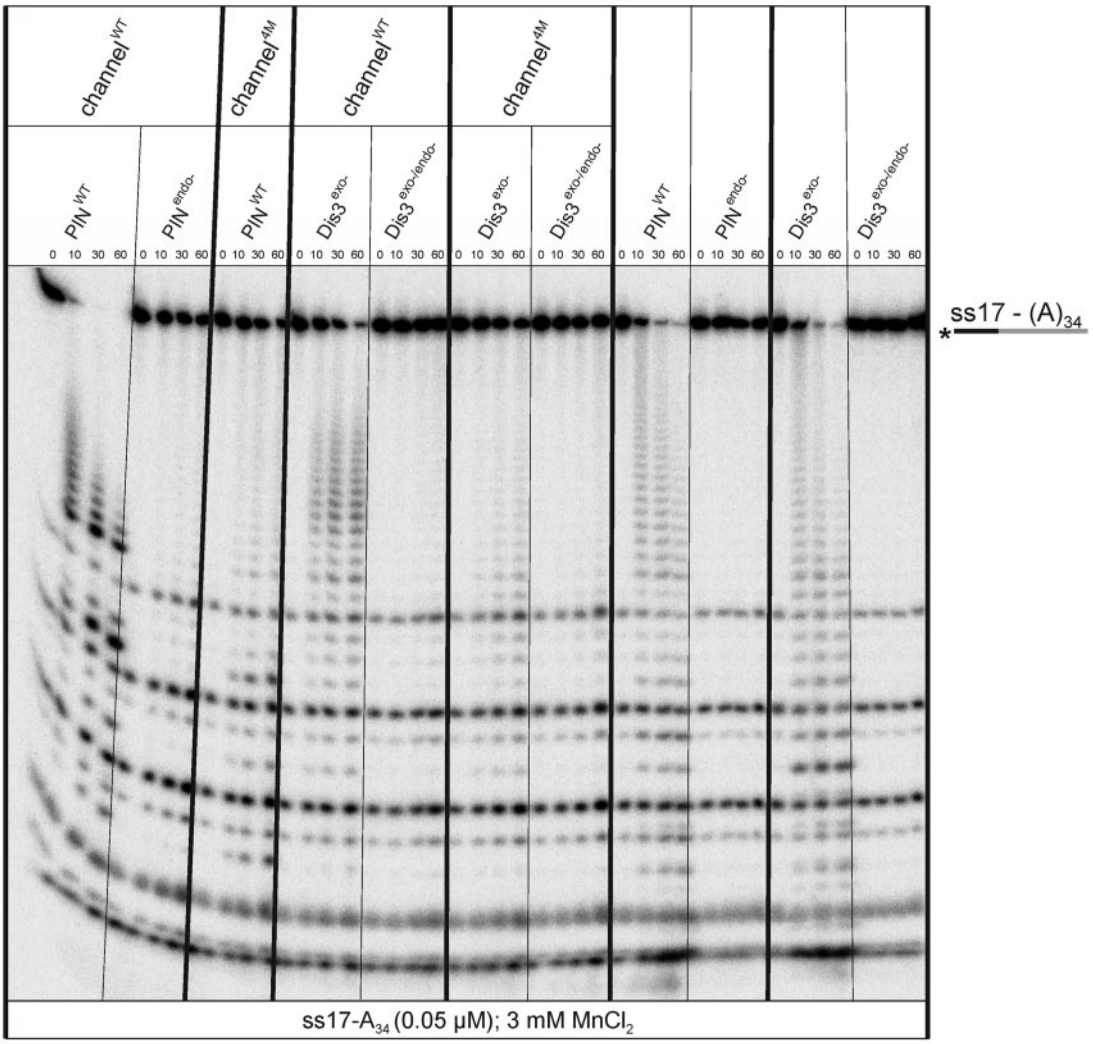

Figure 5. *Rrp41*^{4M} mutation, which blocks the central exosome channel, significantly decreases endoribonucleolytic activity of Dis3 PIN domain. The 5′-labelled ss17-$(A)_{34}$ substrate was incubated in a buffer containing 3 mM manganese with various *in vitro* reconstituted *C. thermophilum* exosome complexes, encompassing either channel^{WT} or channel^{4M}, in conjunction with different versions of PIN domain (PIN^{WT}, PIN^{endo-}) or full-length Dis3 (Dis3^{exo-}, Dis3$^{exo-/endo-}$); parallel assays were done using individual PIN^{WT}, PIN^{endo-}, Dis3^{exo-} and Dis3$^{exo-/endo-}$ proteins. Assays were performed and analysed as described in the Figure 4A legend.

of ds17-$(A)_{34}$ (Figure 7B). We also introduced the same Rrp4 mutations into reconstructed exosomes from *C. thermophilum* (Supplementary Figure S2A) and analysed the exosome activity against single-stranded and structured substrates as described earlier in the text. Again, the effect of *C. thermophilum* Rrp4^{3M} on the degradation of ss17-$(A)_{34}$ (Figure 7C) and ds17-$(A)_{34}$ (Figure 7D) substrates was analogous, meaning the mutation inhibited the activity with a stronger effect on double-stranded substrate. Finally, we reconstituted *C. thermophilum* exosome with both *Rrp4*^{3M} and *Rrp41*^{4M} mutations (Supplementary Figure S2A) and analysed its activity using the same substrates as aforementioned, and we found out that combination of these mutations led to the somewhat synergistic inhibition of exosome activity on both single-stranded and structured substrates (Figures 7C and D, respectively). This indicated that RNA can pass through the central channel of the exosome containing Rrp4^{3M}. Finally, we checked that all reconstructed exosomes were able to unwind partial RNA duplex, leading to release of the complementary strand, as demonstrated in Supplementary Figure S7.

Taking into account the results of biochemical assays presented earlier in the text, we concluded that *Rrp4*^{3M} mutation inhibits exosome activity, particularly against structured substrates, but the observed level of inhibition is rather unlikely to account for the lethal phenotype. Therefore, we further analysed the molecular effects of *Rrp4*^{3M} mutation. First, we checked the intracellular localization of the mutant Rrp4^{3M}, which turned out to be the same as for the WT protein (Figure 8A). Next, we hypothesized that as the only essential exosome cofactor is the RNA helicase Mtr4, the lethality could be caused by the disruption of the interaction between the exosome and Mtr4. However, this was not the case, as co-immunoprecipitation experiments followed by western blot analysis showed similar interaction efficiencies (Figure 8B).

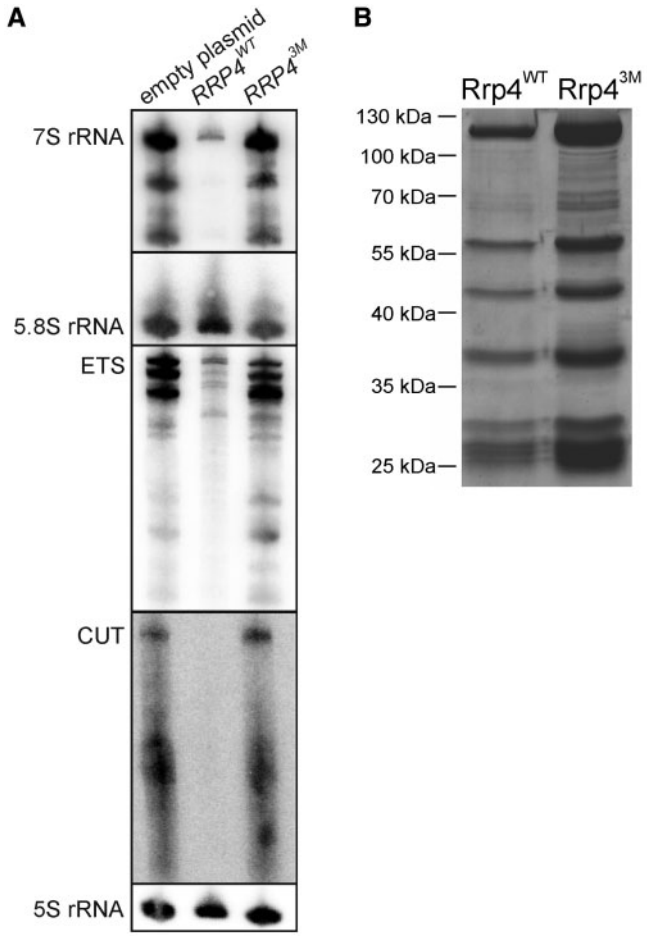

Figure 6. *Rrp4*^{3M} mutation leads to accumulation of typical nuclear exosome substrates, but does not affect assembly of the complex. (**A**) Northern blot analysis of 7S rRNA, 5.8S rRNA, 5′-ETS and CUT in *RRP4* tet-off strains transformed with leucine-marked plasmids containing WT, the 3M version of *RRP4* or empty plasmid as a control grown 20 h in medium without leucine and containing doxycyline. The 5S rRNA was used as a loading control. (**B**) The *Rrp4*^{3M} mutation does not impair exosome assembly. SDS–PAGE analysis of exosomes purified from the *RRP4* tet-off strain transformed with plasmid containing WT or 3M version of *RRP4* with protein A sequence at the C-terminus.

In summary, the only molecular effect of the *Rrp4*^{3M} mutation on the exosome activity we have observed so far is the inhibition, but not inactivation of RNA decay, which seems to be more pronounced for substrates containing double-stranded region than in the case of unstructured RNA molecules; however, the reason for the lethality of such mutation has not been determined.

DISCUSSION

The role of the exosome channel in substrate recruitment

In this study, we analysed the effect of exosome channel blockage by *Rrp41*^{4M} mutation on exosome functions *in vivo* and *in vitro*. We show that in the cytoplasm, when 5′–3′ decay pathways were inactivated, the *Rrp41*^{4M} mutation drastically increased the half lives of all reporter mRNAs. Interestingly, the substrates of NSD, which requires either endo- or exonucleolytic Dis3 activities (27), were also strongly stabilized. This is the first *in vivo* indication that the channel recruits the substrates to the Dis3 in the cytoplasm and that not only exonucleolytic but also endonucleolytic activity of the protein is controlled by the central channel. We also observed accumulation of all tested nuclear exosome substrates: 7S precursor of 5.8S rRNA and 5′-ETS, as well as CUTs in *rrp41*^{4M} mutant strain. Role of the channel in nuclear exosome-mediated RNA hydrolysis is also supported by the very recent publication showing that channel blockage by the introduction of loops in the exosome ring subunits leads to accumulation of CUTs, U4 snRNA and inhibits rRNA processing (23). Curiously, although *Rrp41*^{4M} mutation caused the accumulation of 7S rRNA in the nucleus, the double *Dis3*$^{exo-}$ *Rrp41*^{4M} mutation did not. This is in sharp contrast to the cytoplasmic NSD *PGK1* reporter where we saw synergistic effect of combined *Dis3*$^{exo-}$ and *Rrp41*^{4M} mutations. It is not easy to unequivocally explain this discrepancy, but we are deeply convinced that the major reason is a presence of Rrp6 in the nucleus and absence of this exonuclease in the cytoplasm. Although we were not studying the 11-subunit exosome with Rrp6 *in vitro*, the synthetic lethality of *Rrp41*^{4M} and *Dis3*$^{exo-}$ with *RRP6* deletion in contrast to viability of *rrp41*^{4M} *dis3*$^{exo-}$ double mutant altogether strongly suggests that there exists some unknown compensatory mechanism in *rrp41*^{4M} *dis3*$^{exo-}$ double mutant. This however does not fit the results obtained by Wasmuth and Lima (23), who clearly demonstrate that the *Dis3*$^{exo-}$ mutation very strongly inhibits Rrp6 activity, and this phenotype is partially rescued by channel occlusion.

In contrast to the lethality of the *Dis3*$^{exo-/endo-}$ double mutation (13), the *Rrp41*^{4M} mutation caused only growth defects at elevated temperatures. The most plausible explanation for this discrepancy is the incomplete blockage of the channel by the *Rrp41*^{4M} mutation. This correlates with our *in vitro* results where we found that both exo- and endonucleolytic activities of reconstructed exosomes from *C. thermophilum* were significantly inhibited, but not completely inactivated. Indeed, the longest loops introduced into the ring subunits by Lima's group apparently caused more efficient inhibition of exosome activity than the electrostatic repulsion used by us and caused lethality when introduced into yeast *in vivo* (23).

The inhibition of PIN endonuclease activity by the channel blockage observed both by us and Wasmuth and Lima (23) very strongly suggests that the PIN domain active site is reached through the central channel, although the currently available structural information did not support existence of such path for RNA substrates. The PIN domain active site is exposed to the solvent, thus providing RNA an unlimited access to the catalytic centre without the need of transmission through the entire central channel (9,19,30). The endonucleolytic activity of full-length Dis3^{exo-} in the context of the entire 10-subunit exosome was slightly inhibited by the channel, when compared with Dis3^{exo-} alone (Figure 5 and Supplementary Figure S6), what is in agreement with the results obtained by Wasmuth and Lima (23). We can therefore conclude that an inactive RNB domain

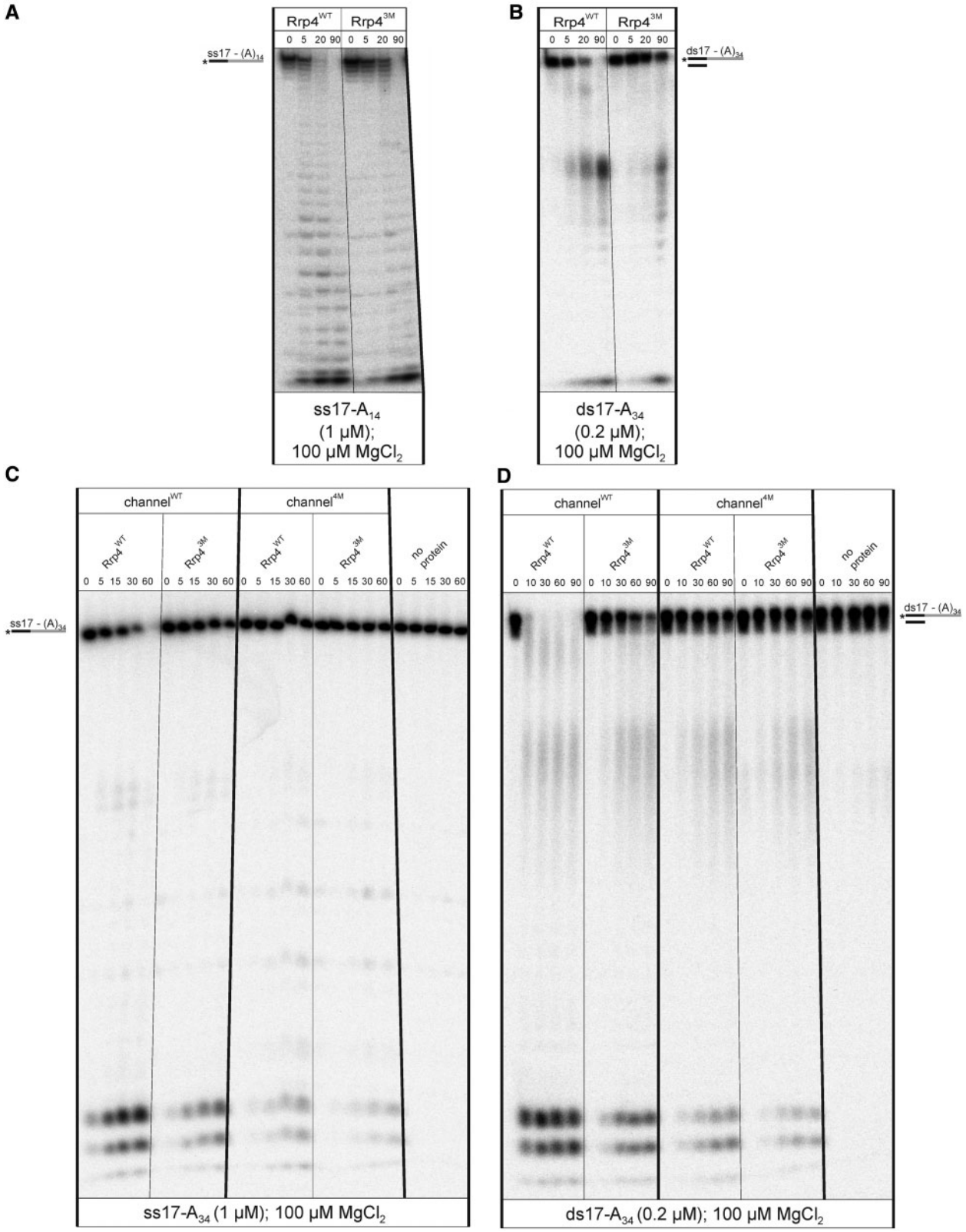

Figure 7. The *Rrp4*^{3M} mutation inhibits degradation of various RNA substrates by both native (A and B) and reconstructed (C and D) exosomes. (**A**) Native exosome containing Rrp4^{3M} protein degrades single-stranded RNA substrate 2–4-fold less efficiently comparing with the wild-type exosome. The 5′-labelled ss17-$(A)_{14}$ substrate was incubated in buffer containing 100 μM magnesium with native yeast 10-subunit exosome complexes containing either wild-type Rrp4 or Rrp4^{3M} (and Dis3^{WT}). Samples were collected at the indicated time points (minutes) and analysed by denaturing PAGE and phosphorimaging. An equal concentration of WT or mutated exosomes and substrate was used for the assay. (**B**) *Rrp4*^{3M} mutation in the native yeast exosome decreases its activity towards structured RNA substrate. ds17-$(A)_{34}$ structured substrate substrate was incubated in buffer containing 100 μM magnesium with native yeast 10-subunit exosome complexes containing either wild-type Rrp4 or Rrp4^{3M} (and Dis3^{WT}). Samples

(continued)

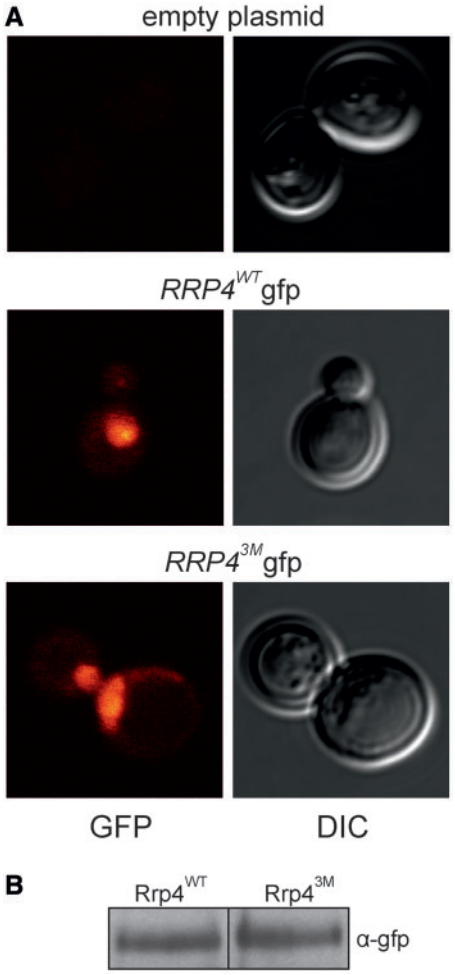

Figure 8. Analysis of Rrp4 localization and its interaction with Mtr4. (**A**) Rrp4^{WT} and Rrp^{3M} have the same cellular localization. *RRP4* tet-off strains transformed with plasmids coding for either gfp-tagged Rrp4^{WT} or Rrp^{3M} were grown in medium with doxycycline for 20 h and localization of the fusion proteins was analysed using fluorescence microscopy. (**B**) The *Rrp4^{3M}* mutation does not disrupt the interaction between the exosome and Mtr4. Extracts from the *RRP4* tet-off strain with gfp-tagged Mtr4 transformed with plasmids containing either WT or 3M *RRP4* tagged with protein A sequence were subjected to immunoglobulin G affinity chromatography followed by western blot analysis using anti-gfp antibodies.

decreases the PIN activity when Dis3 is part of the complex. This inhibition can be explained by competition for the channel, i.e. the RNA substrates that form relatively strong and stable interactions with catalytically inactive RNB domain would occupy the channel and thereby preclude interaction with the PIN domain. Moreover, although endonuclease activity of Dis3 digests the substrate more or less randomly, it acquires some 3′–5′ directionality once bound to the exosome core, further supporting the role of the channel. This phenomenon was also observed by Wasmuth and Lima (23). Interestingly, endonucleolytic activity of the PIN domain was enhanced in our experiment carried out using the reconstructed exosome devoid of the Dis3 S1, CSD and RNB domains (Figure 5 and Supplementary Figure S6). Such analysis was omitted in a study of Wasmuth and Lima, what let the authors suggest that the channel itself inhibits both ribonucleolytic activities of Dis3. On the contrary, our result obtained using reconstituted exosome with PIN domain alone instead of the full-length Dis3 strongly suggests that the channel may increase the endonucleolytic degradation rates, probably by increasing the affinity for substrate, once RNA is not transmitted to preferred exonuclease active site of RNB domain. PIN domain alone has apparently very low affinity towards RNA, and our attempts to detect interactions between the PIN domain and RNA were unsuccessful, what lends further support to the hypothesis that increased activity results from better RNA binding by the exosome core. In general, although Wasmuth and Lima (23) observed stronger inhibition of both Dis3 ribonucleolytic activities by the exosome ring than we did, such a discrepancy may be due to different substrates used in both cases or different sources of the exosome, and it does not change major conclusions of these two independent studies.

In summary, this report characterized the central role of the exosome ring channel in degradation of RNA by both ribonucleolytic activities of Dis3. Further structural studies will be needed to provide additional information about the path that RNA substrates take from the ring to the PIN domain endonuclease active site.

Lethal *Rrp4^{3M}* mutation inhibits digestion of different RNA substrates by Dis3 in the context of the exosome core

In our previous study, we saw that a mutation in conserved basic residues on the surface of Rrp4—*Rrp4^{3M}*—has a lethal phenotype (19). In the present study, we identified the molecular consequences of this mutation. In terms of accumulation of exosome substrates, the *rrp4^{3M}* mutant behaves like a null mutant, but, to our surprise, the substitutions have only moderate effects on exosome activity and do not influence interactions with the RNA helicase Mtr4. The major effect of the *Rrp4^{3M}* mutation on exosome activity, which we were able to identify, was an inhibition of Dis3 activity of both single-stranded RNA molecules and, even more

Figure 7. Continued
were collected at the indicated time points (min) and analysed by denaturing PAGE and phosphorimaging. An equal concentration of WT or mutated exosomes and substrate was used for the assay. (**C**) The 5′-labelled ss17-$(A)_{34}$ substrate was incubated in buffer containing 100 μM magnesium with *in vitro* reconstituted *C. thermophilum* 10-subunit exosome complexes containing either wild-type Rrp4 or Rrp4^{3M} (and Dis3^{WT}) or in the absence of added protein. Samples were collected at the indicated time points (min) and analysed by denaturing PAGE and phosphorimaging. (**D**) ds17-$(A)_{34}$ structured substrate was incubated in buffer containing 100 μM magnesium with *in vitro* reconstituted *C. thermophilum* 10-subunit exosome complexes containing either wild-type Rrp4 or Rrp4^{3M} (and Dis3^{WT}) or in the absence of added protein. Samples were collected at the indicated time points (min) and analysed by denaturing PAGE and phosphorimaging.

significantly, structured substrates. It was recently proposed that during digestion of structured substrates, Dis3 accumulates energy from elastic conformational changes and coupling of hydrolysis and unwinding (31). The unwinding appears in a burst after digestion of ~4 nt. In the context of the entire ring, it is highly probable that when the duplex is positioned at or near Rrp4 rather than the S1 CSD, the transmission of the energy is different. We can hypothesize that changes of basic residues in Rrp4 may interfere with these conformational changes, energy transmission or change the position of RNA that may lead to difficulties in digestion of structured substitutes. Alternatively, disruption of Rrp4 interactions with RNA may inhibit the channelling efficiency, which would have a more pronounced effect on structured substrates. Further studies are needed to fully understand the role of Rrp4 in digestion of structured substrates by the exosome complex.

SUPPLEMENTARY DATA

Supplementary Data are available at NAR Online: Supplementary Tables 1–4, Supplementary Figures 1–7, Supplementary Materials and Methods and Supplementary Reference [32].

ACKNOWLEDGEMENTS

The authors thank Bertrand Seraphin and Roy Parker for yeast strains and plasmids, Aleksander Chlebowski for help with confocal imaging and discussions, Joanna Kufel and members of the AD laboratory for stimulating discussions. A.D. conceived and directed the studies. A.D., K.D. and R.T. designed and analysed the experiments. K.D. performed all experiments in yeast. M.C.-C. cultivated *C. thermophilum* and provided its cDNA. K.K. prepared expression constructs, and K.S. reconstructed the exosome from *C. thermophilum*. K.D. carried out biochemical assays on exosomes purified from *S. cerevisiae*. R.T. performed all *in vitro* experiments on recombinant proteins and reconstituted exosomes from *C. thermophilum*, with the help of K.D. A.D. wrote the manuscript with major contributions from K.D. and R.T.

FUNDING

Polish Ministry of Science and Higher Education [0737/B/P01/2011/40], Foundation for Polish Science Team Programme, co-financed by the EU European Regional Development Fund, the Operational Program Innovative Economy 2007-2013 [TEAM/2008-2/1]. R.T. is the recipient of a scholarship for outstanding young scientists from the Polish Ministry of Science and Higher Education. M.C.-C. is the recipient of a scholarship from European Social Fund [UDA-POKL.04.01.01-00-072/09-00]. Experiments were carried out with the use of CePT infrastructure financed by the European Union—the European Regional Development Fund [Innovative economy 2007–13, Agreement POIG.02.02.00-14-024/08-00]. Funding for open access charge: Foundation for Polish Science Team Programme, co-financed by the EU European Regional Development Fund, the Operational Program Innovative Economy 2007-2013 [TEAM/2008-2/1].

Conflict of interest statement. None declared.

REFERENCES

1. Mitchell,P., Petfalski,E., Shevchenko,A., Mann,M. and Tollervey,D. (1997) The exosome: a conserved eukaryotic RNA processing complex containing multiple 3′→5′ exoribonucleases. *Cell*, **91**, 457–466.
2. Tomecki,R., Drazkowska,K. and Dziembowski,A. (2010) Mechanisms of RNA degradation by the eukaryotic exosome. *Chembiochem*, **11**, 938–945.
3. Allmang,C., Kufel,J., Chanfreau,G., Mitchell,P., Petfalski,E. and Tollervey,D. (1999) Functions of the exosome in rRNA, snoRNA and snRNA synthesis. *EMBO J.*, **18**, 5399–5410.
4. Wang,X., Jia,H., Jankowsky,E. and Anderson,J.T. (2008) Degradation of hypomodified $tRNA_i^{Met}$ *in vivo* involves RNA-dependent ATPase activity of the DExH helicase Mtr4p. *RNA*, **14**, 107–116.
5. Isken,O. and Maquat,L.E. (2007) Quality control of eukaryotic mRNA: safeguarding cells from abnormal mRNA function. *Genes Dev.*, **21**, 1833–1856.
6. Dziembowski,A., Lorentzen,E., Conti,E. and Seraphin,B. (2007) A single subunit, Dis3, is essentially responsible for yeast exosome core activity. *Nat. Struct. Mol. Biol.*, **14**, 15–22.
7. Liu,Q., Greimann,J.C. and Lima,C.D. (2006) Reconstitution, activities, and structure of the eukaryotic RNA exosome. *Cell*, **127**, 1223–1237.
8. Schneider,C., Anderson,J.T. and Tollervey,D. (2007) The exosome subunit Rrp44 plays a direct role in RNA substrate recognition. *Mol. Cell*, **27**, 324–331.
9. Bonneau,F., Basquin,J., Ebert,J., Lorentzen,E. and Conti,E. (2009) The yeast exosome functions as a macromolecular cage to channel RNA substrates for degradation. *Cell*, **139**, 547–559.
10. Butler,J.S. and Mitchell,P. (2011) Rrp6, rrp47 and cofactors of the nuclear exosome. *Adv. Exp. Med. Biol.*, **702**, 91–104.
11. Schneider,C., Leung,E., Brown,J. and Tollervey,D. (2009) The N-terminal PIN domain of the exosome subunit Rrp44 harbors endonuclease activity and tethers Rrp44 to the yeast core exosome. *Nucleic Acids Res.*, **37**, 1127–1140.
12. Schaeffer,D., Tsanova,B., Barbas,A., Reis,F.P., Dastidar,E.G., Sanchez-Rotunno,M., Arraiano,C.M. and van Hoof,A. (2009) The exosome contains domains with specific endoribonuclease, exoribonuclease and cytoplasmic mRNA decay activities. *Nat. Struct. Mol. Biol.*, **16**, 56–62.
13. Lebreton,A., Tomecki,R., Dziembowski,A. and Seraphin,B. (2008) Endonucleolytic RNA cleavage by a eukaryotic exosome. *Nature*, **456**, 993–996.
14. Frazao,C., McVey,C.E., Amblar,M., Barbas,A., Vonrhein,C., Arraiano,C.M. and Carrondo,M.A. (2006) Unravelling the dynamics of RNA degradation by ribonuclease II and its RNA-bound complex. *Nature*, **443**, 110–114.
15. Schaeffer,D., Reis,F.P., Johnson,S.J., Arraiano,C.M. and van Hoof,A. (2012) The CR3 motif of Rrp44p is important for interaction with the core exosome and exosome function. *Nucleic Acids Res.*, **40**, 9298–9307.
16. Tomecki,R., Kristiansen,M.S., Lykke-Andersen,S., Chlebowski,A., Larsen,K.M., Szczesny,R.J., Drazkowska,K., Pastula,A., Andersen,J.S., Stepien,P.P. *et al.* (2010) The human core exosome interacts with differentially localized processive RNases: hDIS3 and hDIS3L. *EMBO J.*, **29**, 2342–2357.
17. Staals,R.H., Bronkhorst,A.W., Schilders,G., Slomovic,S., Schuster,G., Heck,A.J., Raijmakers,R. and Pruijn,G.J. (2010) Dis3-like 1: a novel exoribonuclease associated with the human exosome. *EMBO J.*, **29**, 2358–2367.
18. Chapman,M.A., Lawrence,M.S., Keats,J.J., Cibulskis,K., Sougnez,C., Schinzel,A.C., Harview,C.L., Brunet,J.P., Ahmann,G.J., Adli,M. *et al.* (2011) Initial genome sequencing and analysis of multiple myeloma. *Nature*, **471**, 467–472.

19. Malet,H., Topf,M., Clare,D.K., Ebert,J., Bonneau,F., Basquin,J., Drazkowska,K., Tomecki,R., Dziembowski,A., Conti,E. *et al.* (2010) RNA channelling by the eukaryotic exosome. *EMBO Rep.*, **11**, 936–942.
20. Mnaimneh,S., Davierwala,A.P., Haynes,J., Moffat,J., Peng,W.T., Zhang,W., Yang,X., Pootoolal,J., Chua,G., Lopez,A. *et al.* (2004) Exploration of essential gene functions via titratable promoter alleles. *Cell*, **118**, 31–44.
21. Lorentzen,E., Basquin,J., Tomecki,R., Dziembowski,A. and Conti,E. (2008) Structure of the active subunit of the yeast exosome core, Rrp44: diverse modes of substrate recruitment in the RNase II nuclease family. *Mol. Cell*, **29**, 717–728.
22. Greimann,J.C. and Lima,C.D. (2008) Reconstitution of RNA exosomes from human and *Saccharomyces cerevisiae*: cloning, expression, purification, and activity assays. *Methods Enzymol.*, **448**, 185–210.
23. Wasmuth,E.V. and Lima,C.D. (2012) Exo- and Endoribonucleolytic Activities of Yeast Cytoplasmic and Nuclear RNA Exosomes Are Dependent on the Noncatalytic Core and Central Channel. *Mol. Cell*, **48**, 133–144.
24. Parker,R. (2012) RNA Degradation in *Saccharomyces cerevisiae*. *Genetics*, **191**, 671–702.
25. Dunckley,T. and Parker,R. (1999) The DCP2 protein is required for mRNA decapping in *Saccharomyces cerevisiae* and contains a functional MutT motif. *EMBO J.*, **18**, 5411–5422.
26. Steiger,M.A. and Parker,R. (2002) Analyzing mRNA decay in *Saccharomyces cerevisiae*. *Methods Enzymol.*, **351**, 648–660.
27. Schaeffer,D. and van Hoof,A. (2011) Different nuclease requirements for exosome-mediated degradation of normal and nonstop mRNAs. *Proc. Natl Acad. Sci. USA*, **108**, 2366–2371.
28. van Hoof,A., Frischmeyer,P.A., Dietz,H.C. and Parker,R. (2002) Exosome-mediated recognition and degradation of mRNAs lacking a termination codon. *Science*, **295**, 2262–2264.
29. Amlacher,S., Sarges,P., Flemming,D., van Noort,V., Kunze,R., Devos,D.P., Arumugam,M., Bork,P. and Hurt,E. (2011) Insight into structure and assembly of the nuclear pore complex by utilizing the genome of a eukaryotic thermophile. *Cell*, **146**, 277–289.
30. Wang,H.W., Wang,J., Ding,F., Callahan,K., Bratkowski,M.A., Butler,J.S., Nogales,E. and Ke,A. (2007) Architecture of the yeast Rrp44 exosome complex suggests routes of RNA recruitment for 3' end processing. *Proc. Natl Acad. Sci. USA*, **104**, 16844–16849.
31. Lee,G., Bratkowski,M.A., Ding,F., Ke,A. and Ha,T. (2012) Elastic coupling between RNA degradation and unwinding by an exoribonuclease. *Science*, **336**, 1726–1729.
32. Huh,W.K., Falvo,J.V., Gerke,L.C., Carroll,A.S., Howson,R.W., Weissman,J.S. and O'Shea,E.K. (2003) Global analysis of protein localization in budding yeast. *Nature*, **425**, 686–691.